

Structures and Energies of $[\text{Co}(\text{CO})_n]^m$ ($m = 0, 1+, 1-$) and $\text{HCo}(\text{CO})_n$: Density Functional Studies

Chun-Fang Huo,[†] Yong-Wang Li,[†] Gui-Sheng Wu,[†] Matthias Beller,[‡] and Haijun Jiao^{*,‡,†}

The State Key Laboratory of Coal Conversion, Institute of Coal Chemistry, Chinese Academy of Sciences, Taiyuan 030001, P. R. China, and Institut für Organische Katalyseforschung (IfOK) an der Universität Rostock e.V., Buchbinderstrasse 5-6, 18055 Rostock, Germany

Received: September 26, 2002

Structures and energies of cobalt carbonyls, $[\text{Co}(\text{CO})_n]^m$ ($m = 0, 1+, 1-$) and $\text{HCo}(\text{CO})_n$, have been computed at the B3LYP density functional level of theory. It is found that these complexes prefer less symmetrical structures, and marginal structural deformations can lead to large energetic changes. The calculated bond dissociation energies of $[\text{Co}(\text{CO})_n]^+$ ($n = 1-5$) are in nice agreement with the experiments, and these in turn verify the optimized structures to be the corresponding global energy minima. A spin-allowed dissociation channel is suggested for $[\text{Co}(\text{CO})_5]^+$ with the loss of an equatorial CO to get the excited singlet state of $[\text{Co}(\text{CO})_4]^+$. Furthermore, the bond dissociation energies of $\text{Co}(\text{CO})_n$ ($n = 1-4$), unavailable experimentally, are computed to aid experiments. In addition, novel structures for the most stable triplet ground states of $[\text{Co}(\text{CO})_n]^+$ ($n = 3, 4$) and for the elusive $\text{HCo}(\text{CO})_3$ are proposed. It is found that Co–CO bond dissociation in $\text{HCo}(\text{CO})_n$ ($n = 1-4$) is energetically more favorable than the Co–H homolysis. The structure and stability of formyl complexes, $(\text{HCO})\text{Co}(\text{CO})_3$, have also been discussed.

Introduction

Cobalt carbonyl compounds are important in organometallic synthesis and catalysis.^{1–10} Coordinately unsaturated cobalt carbonyl derivatives are known to be catalytic intermediates,^{11,12} for example, in the important industrial hydroformylation process of long chain aliphatic olefins with $\text{HCo}(\text{CO})_4$ as a precatalyst.^{6,13} They also can serve as models of CO activation on the surfaces of cobalt-based catalysts,⁸ of which Fischer–Tropsch synthesis¹⁴ is one of the most representative examples. Therefore, considerable attention has been attracted both experimentally^{15–27} and theoretically.^{26–34} The first observation of $\text{Co}(\text{CO})_4$ free radical was reported more than 35 years ago, and its possible existence was evidenced by several studies.^{15–18} Using matrix technique, Hanlan¹⁹ isolated and characterized $\text{Co}(\text{CO})_n$ ($n = 1-4$) complexes with infrared, Raman, ultraviolet–visible, and electron spin resonance spectroscopy systematically, and proposed the possible structures on the basis of infrared spectra. Recently, C–O stretch frequencies of $\text{Co}(\text{CO})_n$ ($n = 1-4$) were measured and computed at the density functional level of theory.^{26,32}

Compared to the neutral complexes, both experimental and theoretical studies on the related anions are rare, and these anions are the most interesting species for catalysis, for example, amidocarbonylation. Extended Hückel calculation suggested $[\text{Co}(\text{CO})_4]^-$ to be tetrahedral and $[\text{Co}(\text{CO})_3]^-$ to be planar or nearly planar,²⁸ and the sequential bond dissociation energy of $[\text{Co}(\text{CO})_n]^-$ ($n = 3, 4$) was determined on the basis of energy-resolved collision-induced dissociation.²¹ Recently, matrix infrared spectra and density functional calculations for $[\text{Co}(\text{CO})_n]^-$ ($n = 1-4$) were reported.²⁶

Less attention was also paid to the corresponding cations. Experimentally, sequential bond dissociation energies of $[\text{Co}(\text{CO})_n]^+$ ($n = 1-5$) were determined in collision-induced dissociation experiments, and the possible structures were proposed on the basis of extended Hückel calculations.²⁴ In addition, the recorded infrared spectra of $[\text{Co}(\text{CO})_n]^+$ ($n = 1, 2$) supported by density functional calculations were reported.²⁷ Theoretical calculations on the electronic structures and bond dissociation energies of $[\text{Co}(\text{CO})_n]^+$ ($n = 1, 2$) were carried out by Barnes.³³ Recently, the $[\text{Co}(\text{CO})_4]^+$ formation by dissolution of neutral metal carbonyl clusters in strong acids under CO atmosphere has been reported, and the IR and Raman spectra suggest a trigonal bipyramidal structure for the solvated $[\text{Co}(\text{CO})_4\text{L}]^+$ cation, in which two CO ligands together with a solvent ligand are in the equatorial plane and two axial CO ligands are in nearly linear alignment.²⁵ On the basis of modified extended Hückel theory, the structures of $[\text{Co}(\text{CO})_n]^+$ ($n = 4, 5$) were calculated by Pensak,³⁴ and no detailed theoretical information for $[\text{Co}(\text{CO})_n]^+$ ($n = 3-5$) was known.

$\text{HCo}(\text{CO})_4$, an active amidocarbonylation catalyst, also has been studied both theoretically and experimentally^{35–50} and is found to have a singlet ground state and a C_{3v} symmetrical trigonal bipyramidal structure with hydrogen in the axial position. Although $\text{HCo}(\text{CO})_3$ has been considered as the active hydroformylation catalyst,¹³ its existence was proposed by Wermer⁵¹ only from the IR spectra of $\text{HCo}(\text{CO})_4$ in an argon matrix at low temperature on irradiation. However, $\text{HCo}(\text{CO})_3$ has attracted considerable theoretical interest, and its structure and electronic configuration were studied extensively. These theoretical results differ strongly from each other and are highly dependent on the used models. Thus, no general conclusion for the structure and electronic properties of $\text{HCo}(\text{CO})_3$ could be made on these bases.^{39–43,52,53} The latest density functional study by Ziegler⁴³ showed that the most stable $\text{HCo}(\text{CO})_3$, which can be considered as removal of one equatorial CO ligand from

* To whom correspondence should be addressed. E-mail: hjiao@ifok.uni-rostock.de.

[†] Chinese Academy of Sciences.

[‡] Institut für Organische Katalyseforschung (IfOK) an der Universität Rostock e.V.

HCo(CO)₄, has a singlet ground state in C_s symmetry. He also found that the C_{3v} symmetrical singlet isomer and all possible triplet states are higher in energy. In addition, neither experimental nor theoretical data are known for the lower-coordinated HCo(CO)_n (*n* = 1, 2). More recently, the carbonylation reaction of CH₃Co(CO)₄ has been studied at the density functional level of theory.⁵⁴

In this paper, structures and electronic configurations, as well as C–O stretch frequencies and bond dissociation energies, of [Co(CO)_n]^m (*m* = 0, 1+, 1–) have been investigated with the B3LYP density functional method, and the calculated results are compared with the available experimental values. Excellent agreement between theory and experiment in bond dissociation energy is found for [Co(CO)_n]⁺ (*n* = 1–5). On this basis, the spin-allowed dissociation mechanism for [Co(CO)₅]⁺ has been proposed. Furthermore, the CO bond dissociation energies of the neutral complexes, which are difficult to measure, have been calculated systematically to aid further experimental studies. In addition, the coordination unsaturated neutral hydride complexes, HCo(CO)_n (*n* = 1–3) and HCo(CO)₄, are discussed.

Computational Details

All of the calculations were carried out at the B3LYP density functional level of theory as implemented in the Gaussian 98 program.⁵⁵ The 6-311+G(d) basis sets were used for both carbon and oxygen, while the Wachters–Hay^{56,57} all-electron basis set, using the scaling factors of Raghavachari and Trucks⁵⁸ and including a single polarization function and a set of diffuse functions, was employed for cobalt. The structures of these species were fully optimized, and subsequent frequency calculations verified the optimized structures to be ground states without imaginary frequencies (*N*_{imag} = 0) or transition states with one imaginary frequency (*N*_{imag} = 1) on the potential energy surface (PES) and provided at the same time the zero-point energies (ZPE) and thermal energies. The calculated vibration frequencies were scaled by an empirical factor of 0.9667 deduced from the CO frequency at the same level. The calculated bond dissociation energy includes the corrections of thermal enthalpy (298 K) and the basis set superposition errors (BSSE), which are found to be necessary for bonding-energy calculations of transition metal carbonyl chemistry. For some benchmarks, highly correlated CCSD(T) single-point energies on the B3LYP/6-311+G(d) optimized structures were calculated.⁵⁹ The Wiberg bond indexes and atomic natural charges were calculated with the NBO program,⁶⁰ and these parameters have been applied successfully to characterize the bonding of metal carbonyl complexes and their derivatives by Frenking.⁶¹ The calculated total electronic energies, multiplicity, and number of imaginary frequencies are shown in the Supporting Information.

Results and Discussion

[Co(CO)_n]⁺ (*n* = 1–5). Table 1 lists the calculated C–O stretch frequencies and bond dissociation energies, and the optimized structures are shown in Figure 1. In an earlier theoretical study, Barnes³³ found that both [Co(CO)]⁺ (**1**⁺) and [Co(CO)₂]⁺ (**2**⁺) have linear structures and triplet ground states. We found a linear structure for **2**⁺ as the energy minimum but two minimum structures for **1**⁺. One is the expected linear structure (**1a**⁺), and another one has a slightly bent structure (**1b**⁺) with a Co–C–O bond angle of 179.94°. The Co–C bond in **1a**⁺ (1.989 Å) is longer than that in **1b**⁺ (1.892 Å), while the C–O bond in the former (1.118 Å) is shorter than that in the latter (1.122 Å). This weak bending shortens the Co–C bond

TABLE 1: B3LYP/6-311+G(d) Calculated C–O Stretch Frequency (ν_{CO} , cm⁻¹) and Bond Dissociation Energy (D_0 , kcal/mol) for the Most Stable [Co(CO)_n]⁺ (*n* = 1–5) Compared with the Available Experimental Values

system	ν_{CO}		D_0	
	calcd (exptl ^c)		calcd	exptl ^d
1b ⁺ (C _s) ^a	2188.3 (2165.5)		39.6 (37.3 ^c)	41.5 ± 1.6
2 ⁺ (D _{∞h}) ^a	2176.7 (2168.9)		34.8 (32.3 ^c)	36.4 ± 2.1
3a ⁺ (C _s) ^a	2165.8, 2168.3		18.9	19.6 ± 2.8
4a ⁺ (C _{2v}) ^a	2156.6, 2163.8		18.7	18.0 ± 1.4
4c ⁺ (D _{4h}) ^b	2143.9			
5a ⁺ (D _{3h}) ^b	2133.7, 2150.1		16.7, ^f 7.8 ^g	18.0 ± 1.2

^a Triplet state. ^b Singlet state. ^c Data from ref 27 in parentheses.

^d Data from ref 24. ^e Data from ref 33. ^f Spin-allowed pathway to **4c**⁺.

^g Spin-forbidden pathway to **4a**⁺.

length (0.097 Å) considerably. The Co–C bond length (1.940 Å) of linear **2**⁺ is between those of **1a**⁺ and **1b**⁺.

At B3LYP/6-311+G(d), **1b**⁺ is 8.8 kcal/mol lower in energy than **1a**⁺, and this shows the considerable repulsive interaction between the Co⁺ center and the CO ligand in **1a**⁺. To validate this difference, CCSD(T) single-point energy calculations were carried out. At the CCSD(T)/6-311+G(d) level, **1b**⁺ is 6.9 kcal/mol more stable than **1a**⁺, and this confirms the B3LYP density functional results both qualitatively and quantitatively.

As shown in Table 1, the calculated bond dissociation energies of 39.6 and 34.8 kcal/mol for **1b**⁺ and **2**⁺ are much closer to the experimental (41.5 ± 1.6 and 36.4 ± 2.1 kcal/mol) results than those by Barnes³³ (37.3 and 32.3 kcal/mol, respectively). This indicates that the quality of the basis set and method used in this work is reasonable for cobalt carbonyl chemistry. However, the calculated C–O stretch frequencies for **1b**⁺ and **2**⁺ of 2188.3 and 2176.7 cm⁻¹ are slightly overestimated as compared to the recent experimental values (2165.5 and 2168.9 cm⁻¹).²⁷ In addition, the CO frequency (2216.3 cm⁻¹) of **1a**⁺ is 28 cm⁻¹ higher than that of **1b**⁺ or 50 cm⁻¹ higher than the experimental value.

Apart from the experimental studies, no detailed theoretical calculations for [Co(CO)_n]⁺ (*n* = 3–5) were reported. On the basis of the orbital energy diagrams from extended Hückel method, Goebel²⁴ suggested that [Co(CO)₃]⁺ (**3**⁺) might have a trigonal planar structure (D_{3h}) and a triplet ground state. However, we found two minimum structures, **3a**⁺ (C_s) and **3b**⁺ (D_{3h}) as triplet states, and **3a**⁺ is more stable than **3b**⁺ by 32.3 kcal/mol.

As shown in Figure 1, the structural parameters of **3a**⁺ are very close to those from C_{2v} symmetry, but optimization with constrained C_{2v} symmetry leads to the less stable **3b**⁺. In **3a**⁺, there are two quite different Co–C distances (1.985 and 1.972 Å) and C–Co–C angles (102.52°/102.48° vs 155.00°), and the two Co–C–O are only slightly bent (179.79° and 179.97°). The Co–C bond length in **3b**⁺ (2.088 Å) is longer than those in **3a**⁺. As in the case of **1**⁺, marginal structural deformation results in large energetic change. The change of **3**⁺ (32.3 kcal/mol) is much larger than that of **1**⁺ (8.8 kcal/mol).

In addition, the calculated CO bond dissociation energy of 18.9 kcal/mol for **3a**⁺ agrees reasonably with the experimental value (19.6 ± 2.8 kcal/mol), and this indicates that **3a**⁺ should be the global minimum for [Co(CO)₃]⁺. For **3a**⁺, there are two very close CO stretch bands computed at 2165.8 and 2168.3 cm⁻¹ with an intensity ratio of roughly 1 to 2, and a third band at 2203.6 cm⁻¹ has nearly zero intensity, but no experimental values are available for comparison.

Furthermore, Goebel²⁴ proposed that the D_{4h} square planar structure of [Co(CO)₄]⁺ (**4**⁺) should be the lowest energy isomer

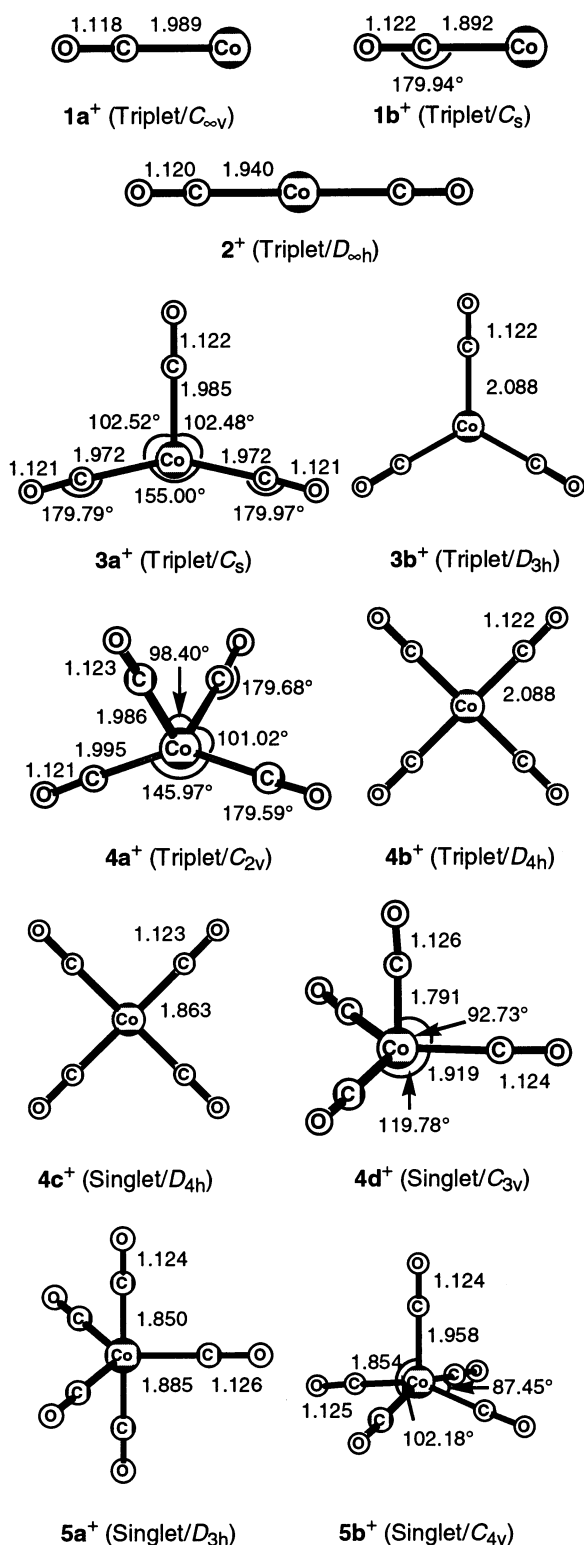


Figure 1. Bond parameters (lengths in Å, angles in deg) for the most stable $[\text{Co}(\text{CO})_n]^+$ ($n = 1-5$).

as triplet ground state, and the singlet state has similar energy. The other nonplanar structures in D_{2d} , C_{4v} , and C_{2v} were higher in energy. However, we found three minimum structures on the PES, that is, the C_{2v} (**4a⁺**) sawhorse geometry as triplet ground state, and the D_{4h} (**4c⁺**) square planar and the C_{3v} (**4d⁺**) trigonal pyramidal structures as singlet states. Structure **4a⁺** is found to be more stable than **4c⁺** and **4d⁺** by 9.5 and 31.3 kcal/mol, respectively. In addition, the proposed D_{4h} (**4b⁺**) planar triplet state with one imaginary frequency is not an energy

minimum and is also 12.2 kcal/mol higher in energy than **4a⁺**. The T_d triplet state (**4e⁺**) not only is less stable (7.1 kcal/mol) but also has two imaginary frequencies. Optimization of the C_{4v} singlet structure leads to the D_{4h} geometry (**4c⁺**), and nonconvergence was found for the D_{2d} structure. Moreover, the calculated bond dissociation energy of the most stable **4a⁺** of 18.7 kcal/mol agrees nearly perfectly with the experimental value (18.0 ± 1.4 kcal/mol), and this indicates that **4a⁺** should represent the global minimum of $[\text{Co}(\text{CO})_4]^+$.

As shown in Figure 1, there are two essentially different C–Co–C angles along the C_2 axis in **4a⁺**. One is more closed (98.40°) and another is more open (145.97°) as compared to the ideal tetrahedral angle. The two Co–C bond lengths (1.986 and 1.995 Å) are close, but they are longer than those of the most stable triplet states $[\text{Co}(\text{CO})_n]^+$ ($n = 1-3$). It is also noteworthy that the Co–C bond length (1.863 Å) of the D_{4h} singlet state (**4c⁺**) is shorter than those of the triplet $[\text{Co}(\text{CO})_n]^+$ ($n = 1-4$). This is mainly because the singlet state has fewer electrons in the antibonding orbital, thereby allowing a stronger bonding.²⁴ The calculated C–O stretch frequency for **4c⁺** of 2143.9 cm^{-1} is lower than those of **4a⁺** of 2156.6 and 2163.8 cm^{-1} , in line with the observed bond-length variations.

For $[\text{Co}(\text{CO})_5]^+$ (**5⁺**), our calculations show its ground state to have the singlet D_{3h} trigonal bipyramidal structure (**5a⁺**), and the C_{4v} symmetry square pyramidal **5b⁺** with one imaginary frequency represents the transition state of pseudorotation. The calculated barrier is 2.1 kcal/mol. The results are in line with the earlier studies by Pensak³⁴ and Goebel.²⁴ As found for **4c⁺**, the Co–C bond lengths are shorter than those of the triplet states (Figure 1). There are two CO vibration modes of 2133.7 (degenerated) and 2150.1 cm^{-1} . Because $[\text{Co}(\text{CO})_4]^+$ has a most stable triplet state (**4a⁺**) and a low-lying excited singlet state (**4c⁺**), there are two ways for the dissociation of singlet **5c⁺** into **4a⁺** or **4c⁺**. One has spin exchange from singlet to triplet, and another has a singlet to singlet transformation.

To reveal where the spin change could occur, Goebel²⁴ compared the sequential bond energies measured with the weak field H_2 . For $[\text{Co}(\text{H}_2)_x]^+$, the bond dissociation energy decreased with the increased number of ligands, and the same trend was also found for $[\text{Co}(\text{CO})_n]^+$ with $n = 1-4$. However, rather than showing a decrease for the fifth CO ligand ($n = 5$), the bond dissociation energy remained fairly constant. This indicated the possible change from triplet to singlet. This analysis plausibly suggested that **5⁺** had a singlet ground state, but it was unclear whether $[\text{Co}(\text{CO})_4]^+$ had a low-lying excited state.²⁴ Our calculations have identified not only the triplet ground state (**4a⁺**) but also the low-lying excited singlet state (**4c⁺**) for $[\text{Co}(\text{CO})_4]^+$.

Because $[\text{Co}(\text{CO})_4]^+$ has a triplet ground state, the dissociation of singlet $[\text{Co}(\text{CO})_5]^+$ could occur via the adiabatic and spin-forbidden channel to form the triplet ground state (**4a⁺**) or along the spin-allowed pathway to form the excited singlet state (**4c⁺**) of $[\text{Co}(\text{CO})_4]^+$. For the spin-allowed pathway, there are two CO for dissociation, that is, the axial one and the equatorial one in **5a⁺**. The axial dissociation will lead to the C_{3v} singlet state (**4d⁺**), while the equatorial alternative will go to the planar D_{4h} singlet state (**4c⁺**).

Goebel²⁴ suggested that if the excitation energy is truly on the order of 5 kcal/mol, the dissociation of $\text{Co}[(\text{CO})_5]^+$ would most likely correspond to the adiabatic process. As shown in Table 1, the bond dissociation energy for the spin-forbidden process leading to **4a⁺** is 7.8 kcal/mol, while that of the spin-allowed pathway for the equatorial CO dissociation leading to the planar D_{4h} excited singlet state (**4c⁺**) is 16.7 kcal/mol, and

TABLE 2: Wiberg Bond Indexes and Natural Charge for the Most Stable $[\text{Co}(\text{CO})_n]^+$ ($n = 1-5$)

system	Co-C	C-O	δ_{Co}	δ_{C}	δ_{O}
1a ⁺ ($C_{\infty v}$) ^a	0.508	2.375	0.936	0.352	-0.288
1b ⁺ (C_s) ^a	0.514	2.370	0.957	0.344	-0.301
2 ⁺ ($D_{\infty h}$) ^a	0.470	2.392	0.772	0.413	-0.299
3a ⁺ (C_s) ^a	0.373	2.367	0.689	0.407	-0.329
	0.419	2.384		0.426	-0.310
4a ⁺ (C_{2v}) ^a	0.372	2.364	0.566	0.440	-0.331
	0.371	2.366		0.438	-0.329
4c ⁺ (D_{4h}) ^b	0.592	2.362	-0.072	0.584	-0.316
5a ⁺ (D_{3h}) ^b	0.599 ^c	2.315 ^c	-0.013	0.595 ^c	-0.331 ^c
	0.415 ^d	2.324 ^d		0.501 ^d	-0.340 ^d

^a Triplet state. ^b Singlet state. ^c Axial CO. ^d Equatorial CO.

TABLE 3: B3LYP/6-311+G(d) Calculated C-O Stretch Frequency (ν_{CO} , cm^{-1}) and CO Bond Dissociation Energy (D_0 , kcal/mol) for the Doublet State $\text{Co}(\text{CO})_n$ ($n = 1-4$) Compared with the Available Literature Values

system	ν_{CO} calcd (exptl)	D_0 calcd (exptl)
1b (C_s)	1958.1 (1957.3 ^a)	23.0 ^c
2b (C_s)	1987.1 (1920.8 ^a)	37.9 (38 \pm 4 ^d)
3a (C_s)	1997.2 (1983.2 ^a)	23.9 (32 \pm 11 ^d)
4 (C_{3v})	2015.4 (2016.6, ^a 2010.7 ^b)	22.0 (30 \pm 12 ^d)
	2027.2 (2023.5, ^a 2028.8 ^b)	
	2095.0 (2107.0 ^b)	

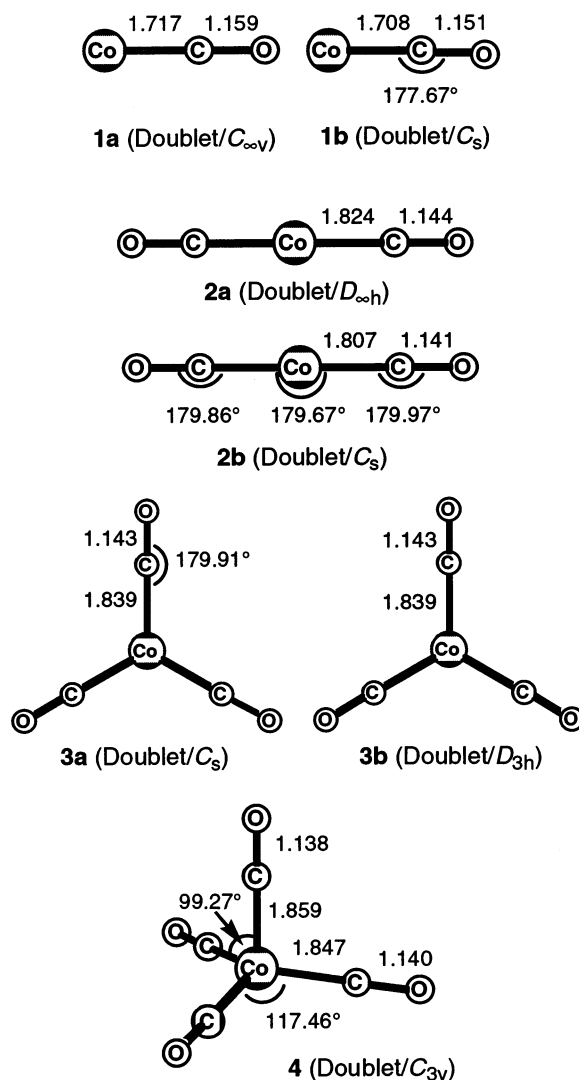
^a Data from ref 26 in parentheses. ^b Data from ref 19 in parentheses.

^c To quartet Co. ^d The interpolated values from ref 21 in parentheses.

the latter is much closer to the measured value of 18.0 ± 1.2 kcal/mol by Goebel.²⁴ The alternative axial CO dissociation energy to **4d**⁺ is 39.7 kcal/mol, which is energetically less favorable as compared to the equatorial way. That the equatorial CO dissociation is much easier than the axial one is also in line with the Co-C bond lengths, and that of the former (1.885 Å) is longer than that of the latter (1.850 Å) in **5a**⁺. On this basis, one might conclude critically that the CO dissociation of $[\text{Co}(\text{CO})_5]^+$ would contact with the spin-allowed path to lose an equatorial CO ligand and get the D_{4h} square planar singlet state of $[\text{Co}(\text{CO})_4]^+$ (**4c**⁺).

Table 2 lists the computed Wiberg bond indexes and atomic natural charges for $[\text{Co}(\text{CO})_n]^+$ ($n = 1-5$) from NBO analysis.⁶⁰ The calculated bond indexes are in line with the variations of the bond lengths, for example, with increased number of CO coordination, the Co-C bond becomes weaker, while the Co-C bond orders in singlet states are larger than those in the triplet states. The difference between the linear and bent $[\text{Co}(\text{CO})]^+$ is also shown clearly, that is, the Co-C bond in **1b**⁺ is stronger than that in **1a**⁺. In line with the Co-C bond lengths and the CO bond dissociation energies, the calculated Wiberg bond index of the equatorial Co-C bond in **5a**⁺ is weaker than the axial one, and therefore, the former should dissociate more easily. In addition, it is noteworthy that the natural charge at the cobalt center varies strongly and it becomes less positive with increased CO coordination. For example, in **1b**⁺, the cobalt center bears nearly the complete positive charge (0.957), while it is only 0.566 in **4a**⁺. In the singlet states, the cobalt center is marginal negatively charged and the total positive charge is distributed over the CO ligands.

Co(CO)_n ($n = 1-4$). Table 3 summarizes the calculated C-O stretch frequencies and bond dissociation energies for all neutral complexes with doublet spin state, and the optimized structures are shown in Figure 2. In line with **1b**⁺, the neutral monocarbonyl complex also has a bent structure (**1b**) with a Co-C-O bond angle of 177.67° , and the linear structure (**1a**) with one imaginary frequency is 21.6 kcal/mol higher in energy. At CCSD(T), **1b** is 17.1 kcal/mol more stable than **1a**, and this

**Figure 2.** Bond parameters (lengths in Å, angles in deg) for the most stable $\text{Co}(\text{CO})_n$ ($n = 1-4$).

confirms the B3LYP result. In addition, the Co-C bond in **1b** (1.708 Å) is shorter than that in **1a** (1.717 Å), indicating a stronger Co and CO interaction in **1b**. However, our finding is in contrast to those by Zhou²⁶ and Ryeng,³² because they found only the linear structure.

As shown in Table 3, the calculated CO frequency of **1b** is nearly identical with the experimental value, and the calculated CO dissociation energy is 23.0 kcal/mol, which is much smaller than the value of 57.5 kcal/mol by Ryeng.³² The good agreement in CO bond dissociation energies between theory and experiment for $[\text{Co}(\text{CO})_n]^+$ ($n = 1-5$, Table 1) gives us the confidence that our computed value of 23.0 kcal/mol for CoCO (**1b**) is reasonable. This energetic difference can mainly be ascribed to the structures employed as reference.

For $\text{Co}(\text{CO})_2$, Ryeng³² found a bent C_{2v} structure with a C-Co-C angle of 152.0° , and it is 7.0 kcal/mol more stable than the linear one, while Zhou²⁶ also found a bent structure but with a much larger C-Co-C angle (171.9°). Our computations show that the linear structure (**2a**) has two degenerated imaginary frequencies and is higher in energy than the slight bent C_s structure (**2b**) by 19.6 kcal/mol. As in the case of CoCO, the structural difference between **2a** and **2b** is marginal, because the C-Co-C and Co-C-O bond angles are 179.67° and 179.86° and 179.97° , and they are very close to 180.00° .

TABLE 4: Wiberg Bond Indexes and Natural Charge for the Most Stable Doublet $\text{Co}(\text{CO})_n$ ($n = 1-4$)

system	Co-C	C-O	δ_{Co}	δ_{C}	δ_{O}
1a ($C_{\infty v}$)	1.109	2.022	0.189	0.326	-0.515
1b (C_s)	1.117	2.070	0.092	0.397	-0.489
2a ($D_{\infty h}$)	0.746	2.164	0.075	0.409	-0.447
2b (C_s)	0.781	2.179	-0.007	0.443	-0.439
3a (C_s)	0.610	2.162	0.340	0.336	-0.450
4 (C_{3v})	0.546 ^a	2.171 ^a	0.184	0.428 ^a	-0.456 ^a
	0.529 ^b	2.172 ^b		0.396 ^b	-0.448 ^b

^a Apical bond. ^b Basal bond.

TABLE 5: B3LYP/6-311+G(d) Calculated C-O Stretch Frequency (ν_{CO} , cm^{-1}) and CO Bond Dissociation Energy (D_0 , kcal/mol) for $[\text{Co}(\text{CO})_n]^-$ ($n = 1-4$) Compared with the Available Experimental Values

system	ν_{CO} calcd (expt ^c)	D_0 calcd (expt ^d)
1a ⁻ (C_s) ^a	1804.4 (1804.0)	17.3
2 ⁻ (C_{2v}) ^b	1776.3 (1768.9)	36.6
	1858.8 (1860.2)	
3a ⁻ (C_{3v}) ^b	1829.1 (1826.9)	47.0 (38.1 \pm 3.9)
4 ⁻ (T_d) ^b	1877.9 (1890.0)	42.4 (39.7 \pm 3.7)

^a Triplet state. ^b Singlet state. ^c Data from ref 26 in parentheses.

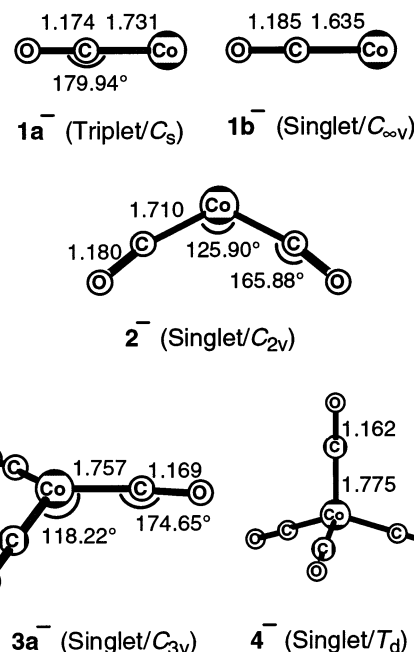
^d Data from ref 21 in parentheses.

It is found that $\text{Co}(\text{CO})_3$ has a C_s trigonal planar structure (**3a**), while the expected D_{3h} conformation (**3b**) is less stable by only 0.1 kcal/mol; and $\text{Co}(\text{CO})_4$ (**4**) is C_{3v} trigonal pyramidal in which the apical Co-C bond is slightly longer than the basal ones. As given in Table 3, nice agreement between the calculated and experimental C-O stretch frequencies is found for CoCO (**1b**), $\text{Co}(\text{CO})_3$ (**3a**), and $\text{Co}(\text{CO})_4$ (**4**), while a large deviation of 66.3 cm^{-1} is found for $\text{Co}(\text{CO})_2$ (**2b**).

In contrast to the cationic systems, no theoretical and experimental determinations for the CO bond dissociation energies of neutral $\text{Co}(\text{CO})_n$ fragments are known. Sunderlin's studies²¹ on the sequential transition metal-carbonyl bond energies illustrated that the relative M-CO bond strength ordering (anion \geq neutral \geq cation) should prevail for the $[\text{M}(\text{CO})_n]^m$ ($n \geq 3$, $m = 1+, 0, 1-$) systems. In terms of this trend, they extrapolated the CO bond dissociation energies for $\text{Co}(\text{CO})_n$ to be 38 ± 4 (**2**), 32 ± 11 (**3**), and 30 ± 12 (**4**) kcal/mol. Unfortunately, because of the large magnitude of the difference in M-CO bond strengths between isoelectronic anions and cations, these deduced values have huge deviation ranges (up to 40%). Nevertheless, our calculations provide the preferable predictions, and the sequence of CO bond dissociation energies is in the order of $\text{Co}(\text{CO})_2 > \text{Co}(\text{CO})_3 \approx \text{CoCO} \approx \text{Co}(\text{CO})_4$ (Table 3), and these systematic computations should aid further experimental investigations.

The computed Wiberg bond indexes and atomic natural charges for $\text{Co}(\text{CO})_n$ ($n = 1-4$) are summarized in Table 4. By comparison with those data in Table 2 of the cationic systems, it is clearly shown that the Co-C bonds in the neutral doublet states are stronger than those in the cationic triplet states. These changes are in line with their bond-length variations, and this is probably because the doublet has only one unpaired electron. In contrast, the natural charge at cobalt does not follow the same trend.

$[\text{Co}(\text{CO})_n]^-$ ($n = 1-4$). Table 5 summarizes the calculated C-O stretch frequencies and bond dissociation energies of these anionic species, and the optimized structures are shown in Figure 3. As $[\text{Co}(\text{CO})]^+$, the $[\text{Co}(\text{CO})]^-$ anion (**1a**⁻) could be an $(\text{sp})^2\text{d}^8$ triplet ground state^{21,26} and is only slightly bent, and the linear singlet state (**1b**⁻) is 23.5 kcal/mol higher in energy. In contrast, $[\text{Co}(\text{CO})_2]^-$ (**2**⁻) has a C_{2v} bent structure as singlet ground state,

**Figure 3.** Bond parameters (lengths in Å, angles in deg) for the most stable $[\text{Co}(\text{CO})_n]^-$ ($n = 1-4$).

and the C-Co-C angle is 125.90° , and the Co-C-O angle is 165.88° , in agreement with the BP86 results.²⁶ The bending of $[\text{Co}(\text{CO})_2]^-$ is due to the repulsive interaction between the electrons in the filled 4s orbital of Co^- ($s^2\text{d}^8$) and the σ -donor orbital of CO, and the 4s electrons are promoted to a hybrid of the 4s and $3d\sigma$ orbital to decrease the repulsion.²¹ Zhou²⁶ has determined the C-O stretch frequencies of these anions and assigned 1804.0 and 1768.9, 1860.2 cm^{-1} to $[\text{Co}(\text{CO})]^-$ and $[\text{Co}(\text{CO})_2]^-$, respectively. Our results are very close to these experimental values, and the largest difference is only 7.4 cm^{-1} . The computed CO dissociation energies are 17.3 kcal/mol for $[\text{Co}(\text{CO})]^-$ and 36.6 kcal/mol for $[\text{Co}(\text{CO})_2]^-$, but no experimental data are available for comparison and validation.

For $[\text{Co}(\text{CO})_3]^-$ (**3**⁻), Elian²⁸ suggested a planar or near-planar geometry, while Zhou²⁶ found a planar (D_{3h}) singlet ground state. However, frequency calculation reveals the D_{3h} structure with one imaginary frequency ($N_{\text{imag}} = 1$) to be not a ground state. Following the imaginary mode, the C_{3v} umbrella structure (**3a**⁻) is identified as the ground state. The energy difference between the D_{3h} (**3b**⁻) and C_{3v} (**3a**⁻) forms is very small (0.1 kcal/mol), but large structural deformation is found. As shown in Figure 3, **3a**⁻ has the Co-C-O bond angle of 174.65° , which shows the bent CO coordination, and the Co center is pyramidal by 5.44° , and the cobalt center is found 0.5 Å over the plane. All of the changes show the quite flat PES, and $[\text{Co}(\text{CO})_3]^-$ can be deformed very easily. These observations are in sharp contrast to those of the cationic and neutral complexes. Furthermore, the calculated C-O stretch frequencies agree nicely with the experimental values, but the CO bond dissociation energy is 9 kcal/mol higher. It is worth noting the large standard deviation of the experimental values. As expected, $[\text{Co}(\text{CO})_4]^-$ (**4**⁻) has a T_d 18-electron singlet state, and the calculated C-O stretch frequency and CO bond dissociation energy are all in line with the available experimental values.

The calculated Wiberg bond indexes and natural charges in Table 6 show that with the increased number of CO coordination the Co-C bond strength for the singlet state decreases and the Co center becomes less negatively charged. Together with the data from Table 2 for the cationic species and Table 4 for the neutral systems, it allows a systematic comparison of bonding

TABLE 6: Wiberg Bond Indexes and Natural Charge for the Most Stable $[\text{Co}(\text{CO})_n]^-$ ($n = 1-4$)

system	Co-C	C-O	δ_{Co}	δ_{C}	δ_{O}
1a⁻ (C_1) ^a	1.003	2.122	-0.515	0.116	-0.601
1b⁻ ($C_{\infty v}$) ^b	1.639	1.813	-0.798	0.464	-0.666
2⁻ (C_{2v}) ^b	1.151	1.882	-0.339	0.294	-0.624
3a⁻ (C_{3v}) ^b	0.835	1.953	-0.205	0.323	-0.588
4⁻ (T_d) ^b	0.660	1.968	-0.076	0.351	-0.581

^a Triplet state. ^b Singlet state.

between cobalt center and CO ligands. On the basis of the traditional Dewar–Chatt–Duncanson model,^{62,63} the metal and CO bonding is considered as CO σ donation and metal d back-donation. This interaction results in the enhancement of the Co–C bond and in the weakening of the CO bond, evidenced by the smaller CO vibration frequencies. From Co^+ to Co and Co^- , the number of metal d electrons increases, and this enables increased d back-donation, and therefore, the Co–C bonds become stronger and the CO ones weaker. As shown in Figures 1 and 3, the Co–C bonds are longer in the cationic systems than those in the anionic species, while the CO bonds show the reversed order. For example, the Co–C bond lengths (1.986, 1.995 Å) in **4a⁺** are the longest, while that of **4⁻** is the shortest (1.775 Å), and those (1.847, 1.859 Å) of **4** are in between. These bond length changes are also supported by the calculated bond orders and the CO vibration frequencies.

HCo(CO)_n ($n = 1-4$). Apart from the neutral and charged cobalt carbonyl complexes, it is also interesting to study the hydride complexes, $\text{HCo}(\text{CO})_n$, because $\text{HCo}(\text{CO})_4$ has been considered as a precatalyst in the important industrial hydroformylation processes.^{9,10} Because of the diverse properties of structures and electronic configurations of the carbonyl complexes, one might also expect the same complexity of these hydrides.

Because all of the most stable monocarbonyl complexes have high-spin states or bent structures, $\text{HCo}(\text{CO})$ (**1-H**) is expected to be bent. Indeed, we found a linear (**1c-H**) and a bent (**1d-H**) singlet state for $\text{HCo}(\text{CO})$ on the PES, and **1d-H** is more stable than **1c-H** by 18.0 kcal/mol. In addition, we also found a bent triplet state (**1b-H**), which is more stable than the linear triplet state (**1a-H**) by 9.8 kcal/mol and than the singlet state **1d-H** by 30.4 kcal/mol. This indicates that the triplet state (**1b-H**) is the most stable isomer. The large structural difference between **1b-H** and **1d-H** is shown in Figure 4. For example, in **1d-H**, the C–Co–H bond angle is 88.21° and the O–C–Co angle of 175.70° indicates a slightly bent substructure. The Co–H and Co–C bonds of the **1b-H** (1.580 vs 1.863 Å) are longer than those of **1d-H** (1.462 vs 1.694 Å), while the C–O bond in the former (1.140 Å) is shorter than that in the latter (1.152 Å).

For $\text{HCo}(\text{CO})_2$, the planar C_{2v} singlet structure (**2a-H**), in which both hydrogen and CO ligands have the same orientation, has one imaginary frequency and is therefore not an energy minimum. The imaginary mode indicates an out-of-plane movement of the hydrogen atom, and this leads to a nonplanar C_s structure as minimum (**2c-H**). Although the vibration barrier is only 0.4 kcal/mol, large structural changes are found. In addition, a planar C_s triplet state (**2b-H**) is found as energy minimum on the PES and is more stable than **2c-H** by 8.8 kcal/mol. This difference is much smaller than that of $\text{HCo}(\text{CO})$. This indicates that the second CO coordination reduces the energy gap between singlet and triplet considerably.

For $\text{HCo}(\text{CO})_3$, the controversial structures and electronic configurations were found theoretically. For example, Daniel⁵² and Antolovic^{39,41} found a C_{3v} triplet ground state, while Veillard⁵³ showed a more stable singlet ground state. In a density

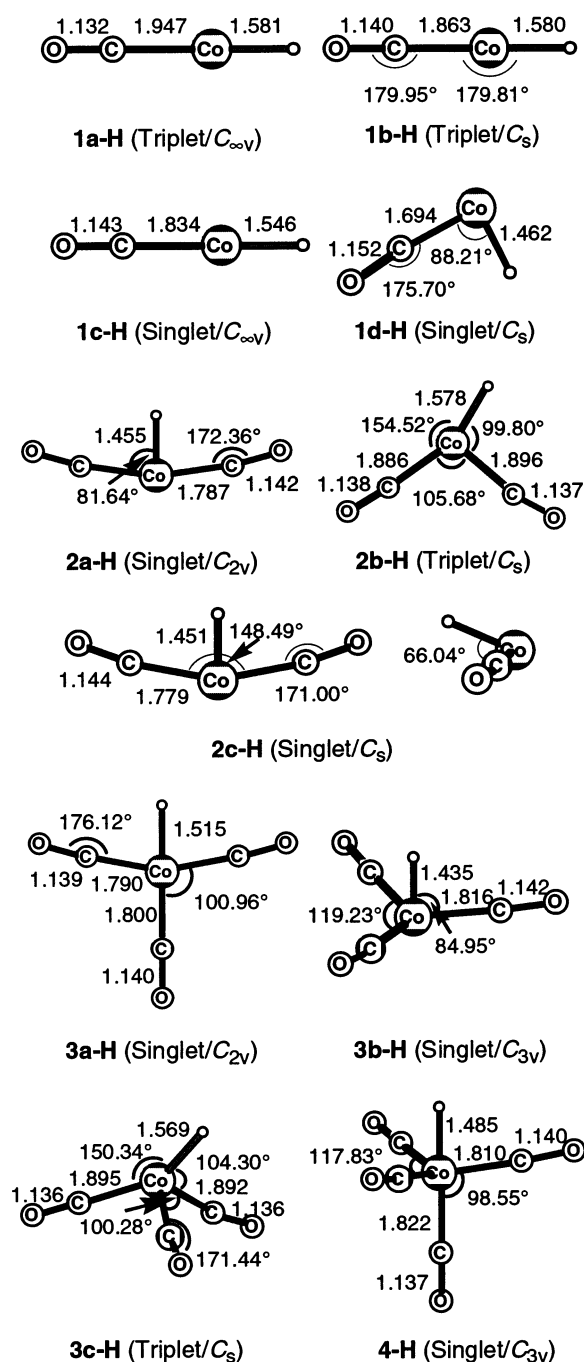


Figure 4. Bond parameters (lengths in Å, angles in deg) for the most stable $\text{HCo}(\text{CO})_n$ ($n = 1-4$).

functional study with local density approximation, Ziegler⁴³ concluded that the most stable ground state of $\text{HCo}(\text{CO})_3$ has a singlet configuration in C_s symmetry and all other possible singlet and triplet states are higher in energy.

In agreement with Ziegler,⁴³ we also found $\text{HCo}(\text{CO})_3$ to have a most stable singlet state. However, we found that the most stable singlet state has a planar C_{2v} structure (**3a-H**) with hydrogen along the C_2 axis, and the Co center has planar tetracoordination as shown in Figure 4, while Ziegler showed a C_s symmetrical form in which the hydrogen is out of the plane. Because of this difference, we took the Ziegler structure as initial geometry, and the B3LYP optimization led to **3a-H**.

In addition, the energy difference between the C_{2v} planar (**3a-H**) and the C_{3v} (**3b-H**) singlet states is 10.4 kcal/mol, which is larger than that of 8.1 kcal/mol by Ziegler. This indicates

TABLE 7: B3LYP/6-311+G(d) Calculated C–O Stretch Frequency (ν_{CO} , cm^{-1}), CO Bond Dissociation Energy (D_0 , kcal/mol) and Co–H Homolytic Dissociation for $\text{HCo}(\text{CO})_n$ ($n = 1-4$) Compared with the Available Experimental Values

system	ν calcd (exptl)	Co–CO	Co–H
1b-H (C_s)	1732 (Co–H) 2053	31.1, 29.3 ^d	66.8
2b-H (C_s)	1707 (Co–H) 2028, 2081	16.7	64.3
3a-H (C_{2v})	1844 (Co–H) 2023 (2018 ^a) 2031 (2025 ^a) 2102	36.5 ^c 28.1 ^d	50.4
4-H (C_{3v})	2030 (2034.1 ^b) 2050 (2058.9 ^b) 2105 (2120.8 ^b)	25.7, ^e 36.3 ^f (12.9 ^g)	54.9 (54.3 ^h ; 66.9 ⁱ)
6b (C_s)	2844 (H–C) 2081, 2022, 1996 (CO) 1677 (η^2 , O=CH)		

^a Data from ref 51 in parentheses. ^b Data from ref 35 in parentheses. ^c Spin-allowed pathway. ^d Spin-forbidden pathway. ^e Loss of equatorial CO. ^f Loss of axial CO. ^g Data from ref 50 in parentheses. ^h Data from ref 48 in parentheses (equilibrium studies in the gas phase). ⁱ Data from ref 49 in parentheses (electrochemical in conjunction with acidity measurement).

that the energy difference between our C_{2v} and Ziegler's C_s structure is not very large. We also found a triplet state (**3c-H**) in C_s symmetry with a tetrahedral Co center, but it is 9.0 kcal/mol higher in energy than **3a-H**. At this stage, it is worth noting that the third coordination of CO has reversed the order of the energy gap between singlet and triplet and the singlet state is more stable than the triplet state.

Ziegler⁴³ assigned the experimentally detected two C–O stretch frequencies at 2018 and 2025 cm^{-1} as a possible combination of C_s and C_{3v} structures. However, we found only one degenerated CO mode of 2066.7 cm^{-1} with high intensity for the C_{3v} structure (**3b-H**) and two CO bands at 2022.8 and 2031.3 cm^{-1} for the most stable C_{2v} structure (**3a-H**), and they are close to the values of 2018 and 2025 cm^{-1} found experimentally. It is worth noting that the calculated relative intensity of nearly 2 to 1 for **3a-H** is roughly comparable to the observed ratio.⁵¹ In addition, the detected band at 485 cm^{-1} might be ascribed to the Co–C stretch modes, and analysis shows that the Co–C stretch frequency has negligible intensity in $\text{HCo}(\text{CO})_4$, while that in $\text{HCo}(\text{CO})_3$ increases somewhat, but it is still much lower than those of CO modes. On the basis of this and of the relative energy, one can conclude that the planar C_{2v} **3a-H** represents the only structure for $\text{HCo}(\text{CO})_3$ as the most stable singlet state and that the existence of the expected C_{3v} isomer during the CO dissociation of $\text{HCo}(\text{CO})_4$ can be ruled out.

The formation of $\text{HCo}(\text{CO})_3$ during the photolysis in a low-temperature matrix proposed by Wermer⁵¹ was supported by Sweany.^{35,64,65} In addition, Sweany also observed the Co–H bond homolysis, evidenced by the electron spin experiment, and the related photolysis in CO matrix yielding formal radical (HCO^*). On this basis, he ascribed the new IR bands during the photolysis to the formation of $\text{Co}(\text{CO})_4$. As given in Tables 3 and 7, both the calculated and experimentally detected C–O stretching frequencies for $\text{Co}(\text{CO})_4$ and $\text{HCo}(\text{CO})_3$ are too close together to make any conclusive assignments.

To compare these results, we computed the energies of Co–CO dissociation and Co–H bond homolysis for $\text{HCo}(\text{CO})_3$. As shown in Table 7, the CO dissociation energies of 25.7 or 36.6 kcal/mol for the loss of the equatorial or axial CO are much

smaller than that (54.9 kcal/mol) of Co–H homolysis in $\text{HCo}(\text{CO})_4$, in line with the available experimental data in the literature and with the computational results by Ziegler.⁴³ That CO dissociates more easily than Co–H is also found in other $\text{HCo}(\text{CO})_n$ complexes. Therefore, CO dissociation is more favored energetically than Co–H homolysis. Because there is no spin change during the dissociation of **4-H** and **3a-H** is more stable than **3b-H** by 10.4 kcal/mol, equatorial CO dissociation should be the only energetically favored pathway and formation of the C_{3v} symmetrical **3b-H** can be ruled out, in agreement with the analysis of C–O stretch frequencies.

In addition to $\text{HCo}(\text{CO})_4$ (**4-H**) and $\text{HCo}(\text{CO})_3$ (**3-H**), we are also interested in the structure and stability of the most stable formyl(tricarbonyl)cobalt, $(\text{HCO})\text{Co}(\text{CO})_3$ (**6**), which has been proposed as an intermediate in substitution reactions and analyzed theoretically on the basis of the Hartree–Fock–Slater (HFS) method.⁴² Structure **6** is an isomer of $\text{HCo}(\text{CO})_4$ but has the same coordination number as $\text{HCo}(\text{CO})_3$. For the structures of **6**, we used the same procedure as that for $\text{HCo}(\text{CO})_3$, deduced from the removal of the axial and equatorial CO ligands of $\text{HCo}(\text{CO})_4$.

The trigonal pyramidal form (**6a**), considered as the removal of the axial CO ligand from trigonal bipyramidal $(\text{HCO})\text{Co}(\text{CO})_4$,⁴² is a minimum structure on the PES but higher in energy than the form (**6b**) deduced from the removal of the equatorial CO by 4.9 kcal/mol. Because our most stable $\text{HCo}(\text{CO})_3$ has a planar structure (**3a-H**), planar $(\text{HCO})\text{Co}(\text{CO})_3$ (**6c**) was also considered. However, **6c** (C_s) has two imaginary frequencies ($N_{\text{imag}} = 2$) on the PES and therefore does not represent energy minimum structure. The first negative mode indicates the rotation of the formyl group. Further optimization following this mode leads to the minimum structure (**6b**) in C_s symmetry with two equatorial and one axial carbonyl groups and an additional formyl group in η^2 coordination. The second negative mode is the out-of-plane deformation, and further optimization leads to the trigonal pyramidal form (**6a**). The corresponding triplet states of **6a** and **6b** are higher in energy by 9.9 and 11.1 kcal/mol, respectively.

In comparison with $\text{HCo}(\text{CO})_4$ (**4-H**), the most stable formyl complex (**6b**) is much higher in energy by 23.4 kcal/mol. The special stability of **6b** can be ascribed to the formation of η^2 coordination. As shown in Figure 5, the Co–O distance is 2.405 Å and the Co–CO(H) has an angle of 100.62°, which is smaller than that of the Ziegler structure (107°). The computed vibration frequencies with the characteristic formyl C–H (2844 cm^{-1}) and η^2 O=CH (1677 cm^{-1}) are given in Table 7.

It is also worth noting that structure **6d**, the most stable formyl complex by Ziegler,⁴² has one imaginary frequency on the PES and the negative mode shows the rotation of the $\text{Co}(\text{CO})_3$ moiety. Further optimization following the negative mode converges to our most stable structure **6b**. On the other hand, **6d** is 4.6 kcal/mol higher in energy than **6b**. This is in sharp contrast to the results by Ziegler, who found that both **6d** and **6b** were minimum structures and **6d** was more stable than **6b** by 8.4 kcal/mol at the HFS level.⁴² In addition, HFS method did not find the structure of **6b** with η^2 formyl coordination. As shown in Figure 5, we found both **6b** and **6d** favoring η^2 formyl coordination, and this reflects the effect of electron correlation on the structure and stability.

As in the dissociation process of $[\text{Co}(\text{CO})_5]^+$, there are also spin-allowed (36.5 kcal/mol) and spin-forbidden (28.1 kcal/mol) pathways for $\text{HCo}(\text{CO})_3$ (**3a-H**). The spin-allowed pathway with the loss of the axial CO leads to the formation of the low-lying excited singlet state (**2c-H**), while the spin-forbidden alternative

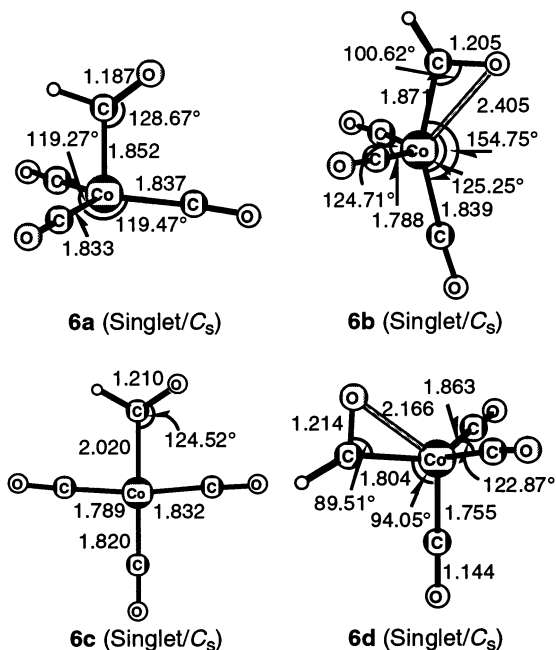


Figure 5. Bond parameters (lengths in Å, angles in deg) for the most stable formyl complex (HCO)Co(CO)₃ (6).

TABLE 8: Wiberg Bond Indexes and Natural Charge for the Most Stable HCo(CO)_n (n = 1–4)

system	Co–C	Co–H	δ_{Co}	δ_{H}
1b-H (C _s) ^a	0.693	0.574	0.623	–0.520
1d-H (C _s) ^b	1.189	0.903	0.131	–0.126
2b-H (C _s) ^a	0.484, 0.557	0.488	0.608	–0.455
2c-H (C _s) ^b	0.789	0.813	0.014	–0.026
3a-H (C _{2v}) ^b	0.670, ^c 0.663 ^d	0.490	–0.200	–0.108
4-H (C _{3v}) ^b	0.559, ^c 0.528 ^d	0.462	–0.142	0.040
6b (C _s)	0.596, ^c 0.655 ^d 0.604 ^e	0.179 ^f		

^a Triplet state. ^b Singlet state. ^c Axial CO. ^d Equatorial CO. ^e Formyl carbon. ^f Formyl oxygen.

with the loss of the equatorial CO leads to the formation of the most stable triplet state (**2b-H**).

Table 8 summarizes some selected Wiberg bond indexes and natural charge. Only in the most stable triplet states (**1b-H**, **2b-H**), the cobalt center is positively charged and hydrogen has negative charge. In the most stable singlet states, both cobalt and hydrogen are nearly neutral. The η^2 formyl coordination is also reflected.

Conclusion

High-level B3LYP/6-311+G(d) density functional investigations into the electronic structures and energies of cobalt carbonyls [Co(CO)_n]^m ($m = 1+, 0, 1-$) and their hydride HCo(CO)_n complexes were carried out systematically. It is found that these complexes prefer less symmetrical structures as the most stable states and marginal structural deformations have large energetic consequence.

The computed C–O stretch frequencies and bond dissociation energies for [Co(CO)_n]⁺ ($n = 1-5$) agree nearly perfectly with the available experimental data. This nice agreement in turn verifies the novel structures for the most stable triplet [Co(CO)₃]⁺ and [Co(CO)₄]⁺ as the global minima. Furthermore, we conclude that [Co(CO)₅]⁺ dissociates via a spin-allowed pathway with the loss of an equatorial CO to get the low-lying excited singlet state [Co(CO)₄]⁺. The proposed novel structures

for the most stable triplet states of [Co(CO)₃]⁺ and [Co(CO)₄]⁺ are C_s and C_{2v} symmetrical.

On the basis of the calculated results for [Co(CO)_n]⁺, the bond dissociation energies of Co(CO)_n ($n = 1-4$), which are difficult to access experimentally, also have been computed, and these results should aid further experimental investigation.

Moreover, a new planar structure as the most stable isomer has been computed for the elusive HCo(CO)₃, and the formation of the C_{3v} symmetrical isomer can be ruled out on the basis of the CO frequencies, bond dissociation energies, and also their energy difference. As in case of [Co(CO)₅]⁺, there are also spin-allowed and spin-forbidden CO dissociation pathways for HCo(CO)₃. It is also found that CO dissociation is energetically more favorable than Co–H homolysis, in agreement with the experiment.

Acknowledgment. This work was supported by Chinese Academy of Sciences (20029908), the National Natural Science Foundation China, and the Natural Science Foundation of the Shanxi Province, China. The support of Alexander von Humboldt Foundation (to Y.-W. Li) is also gratefully acknowledged.

Supporting Information Available: Total electronic energies, zero-point energies, multiplicity, and number of imaginary frequencies for all systems. This material is available free of charge via the Internet at <http://pubs.acs.org>.

References and Notes

- Krafft, M. E.; Bonaga, L. V. R.; Wright, J. A.; Hirose, C. *J. Org. Chem.* **2002**, *67*, 1233.
- Cornils, B.; Herrmann, W. A. *Applied Homogeneous Catalysis with Organometallic Compounds*; VCH–Wiley: New York, 1996.
- Parshall, G. W.; Ittel, S. D. *Homogeneous Catalysis*; Wiley-Interscience: New York, 1992.
- Herrmann, W. A.; Cornils, B. *Angew. Chem., Int. Ed. Engl.* **1997**, *36*, 1048.
- Cotton, F. A.; Wilkinson, G.; Murillo, C. A.; Bochmann, M. *Advanced Inorganic Chemistry*, 6th ed.; Wiley: New York, 1999.
- Torrent, M.; Solà, M.; Frenking, G. *Chem. Rev.* **2000**, *100*, 439.
- Tremblay, B.; Alikhani, M. E.; Manceron, L. *J. Phys. Chem. A* **2001**, *105*, 11388.
- Zhou, M.-F.; Andrews, L.; Bauschlicher, C. W. *Chem. Rev.* **2001**, *101*, 1931.
- Beller, M.; Krauter, J. G. E. *J. Mol. Catal. A* **1999**, *143*, 31.
- Beller, M.; Cornils, B.; Frohning, C. D.; Kohlpaintner, C. W. *J. Mol. Catal. A* **1995**, *104*, 17.
- Chalk, A. J.; Harrod, J. F. *Adv. Organomet. Chem.* **1968**, *6*, 119.
- Whyman, R. *J. Organomet. Chem.* **1974**, *81*, 97.
- Heck, R. F.; Breslow, D. S. *J. Am. Chem. Soc.* **1961**, *83*, 4023.
- Fischer, F.; Tropsch, H. *Brennst.-Chem.* **1923**, *4*, 276.
- Keller, H. J.; Wawersik, B. W. *Z. Naturforsch.* **1965**, *206*, 938.
- Bidinosti, D. R.; McIntyre, N. S. *Chem. Commun.* **1967**, 1.
- Crichton, O.; Poliakoff, M.; Rest, A. J.; Turner, J. J. *J. Chem. Soc., Dalton Trans.* **1973**, 1321.
- Fieldhouse, S. A.; Fullam, B. W.; Neilson, G. W.; Symons, M. C. R. *J. Chem. Soc., Dalton Trans.* **1974**, 567.
- Hanlan, L. A.; Huber, H.; Kundig, E. P.; McGarvey, B. R.; Ozin, G. A. *J. Am. Chem. Soc.* **1975**, *97*, 7054.
- Edgell, W. F.; Lyford, J.; Barbetta, A.; Jose, C. I. *J. Am. Chem. Soc.* **1971**, *93*, 6403.
- Sunderlin, L. S.; Wang D.-N.; Squires, R. R. *J. Am. Chem. Soc.* **1993**, *115*, 12060.
- Winters, R. E.; Kiser, R. W. *J. Phys. Chem.* **1965**, *69*, 1618.
- Saalfeld, F. E.; McDowell, M. V.; Gondal, S. K.; MacDiarmid, A. G. *J. Am. Chem. Soc.* **1968**, *90*, 3684.
- Goebel, S.; Haynes, C. L.; Khan, F. A.; Armentrout, P. B. *J. Am. Chem. Soc.* **1995**, *117*, 6994.
- Xu, Q.; Inoue, S.; Souma, Y.; Nakatani, H. *J. Organomet. Chem.* **2000**, *606*, 147.
- Zhou, M.-F.; Andrews, L. *J. Phys. Chem. A* **1998**, *102*, 10250.
- Zhou, M.-F.; Andrews, L. *J. Phys. Chem. A* **1999**, *103*, 7773.
- Elián, M.; Hoffmann, R. *Inorg. Chem.* **1975**, *14*, 1058.
- Burdett, J. K. *J. Chem. Soc., Faraday Trans. II* **1974**, *70*, 1599.
- Fournier, R. *J. Chem. Phys.* **1993**, *99*, 1801.
- Adamo, C.; Lelj, F. *J. Chem. Phys.* **1995**, *103*, 10605.

- (32) Ryeng, H.; Gropen, O.; Swang, O. *J. Phys. Chem. A* **1997**, *101*, 8956.
- (33) Sweany, R. L.; Rosi, M.; Bauschlicher, C. W. *J. Chem. Phys.* **1990**, *93*, 609.
- (34) Pensak, D. A.; McKinney, R. J. *Inorg. Chem.* **1979**, *18*, 3407.
- (35) Sweany, R. L. *Inorg. Chem.* **1980**, *19*, 3512.
- (36) (a) Edgell, W. F.; Magee, C.; Gallup, G. *J. Am. Chem. Soc.* **1956**, *78*, 4185. (b) Edgell, W. F.; Gallup, G. *J. Am. Chem. Soc.* **1956**, *78*, 4188. (c) Cotton, F. A. *J. Am. Chem. Soc.* **1958**, *80*, 4425. (d) Edgell, W. F.; Summitt, R. *J. Am. Chem. Soc.* **1961**, *83*, 1172.
- (37) McNeill, E. A.; Scholer, F. R. *J. Am. Chem. Soc.* **1977**, *99*, 6243.
- (38) Bellagamba, V.; Ercoli, R.; Gamba, A.; Suffritti, G. B. *J. Organomet. Chem.* **1980**, *190*, 381.
- (39) Antolovic, D.; Davidson, E. R. *J. Am. Chem. Soc.* **1987**, *109*, 977.
- (40) Antolovic, D.; Davidson, E. R. *J. Am. Chem. Soc.* **1987**, *109*, 5828.
- (41) Antolovic, D.; Davidson, E. R. *J. Chem. Phys.* **1988**, *88*, 4967.
- (42) Versluis, L.; Ziegler, T.; Baerends, E. J.; Ravenek, W. *J. Am. Chem. Soc.* **1989**, *111*, 2018.
- (43) Ziegler, T.; Cavallo, L.; Bérces, A. *Organometallics* **1993**, *12*, 3586.
- (44) Ribbing, C.; Daniel, C. *J. Chem. Phys.* **1994**, *100*, 6591.
- (45) Folga, E.; Ziegler, T. *J. Am. Chem. Soc.* **1993**, *115*, 5169.
- (46) Jonas, V.; Thiel, W. *J. Chem. Phys.* **1996**, *105*, 3636.
- (47) Zhao, Y.; Kühn, O. *Chem. Phys. Lett.* **1999**, *302*, 7.
- (48) Connor, J. A. *Top. Curr. Chem.* **1977**, *71*, 71.
- (49) (a) Tilset, M.; Parker, V. D. *J. Am. Chem. Soc.* **1989**, *111*, 6711. (b) Tilset, M.; Parker, V. D. *J. Am. Chem. Soc.* **1990**, *112*, 2843.
- (50) Ungváry, F.; Markó, L. *J. Organomet. Chem.* **1969**, *20*, 205.
- (51) Wermer, P.; Ault, B. S.; Orchin, M. *J. Organomet. Chem.* **1978**, *162*, 189.
- (52) Daniel, C.; Hyla-Kryspin, I.; Demuynck, J.; Veillard, A. *Nouv. J. Chim.* **1985**, *9*, 582.
- (53) Veillard, A.; Daniel, C.; Rohmer, M.-M. *J. Phys. Chem.* **1990**, *94*, 5556.
- (54) Goh, S. K.; Marynick, D. S. *Organometallics* **2002**, *21*, 2262.
- (55) Frisch, M. J.; Trucks, G. W.; Schlegel, H. B.; Scuseria, G. E.; Robb, M. A.; Cheeseman, J. R.; Zakrzewski, V. G.; Montgomery, J. A., Jr.; Stratmann, R. E.; Burant, J. C.; Dapprich, S.; Millam, J. M.; Daniels, A. D.; Kudin, K. N.; Strain, M. C.; Farkas, O.; Tomasi, J.; Barone, V.; Cossi, M.; Cammi, R.; Mennucci, B.; Pomelli, C.; Adamo, C.; Clifford, S.; Ochterski, J.; Petersson, G. A.; Ayala, P. Y.; Cui, Q.; Morokuma, K.; Malick, D. K.; Rabuck, A. D.; Raghavachari, K.; Foresman, J. B.; Cioslowski, J.; Ortiz, J. V.; Stefanov, B. B.; Liu, G.; Liashenko, A.; Piskorz, P.; Komaromi, I.; Gomperts, R.; Martin, R. L.; Fox, D. J.; Keith, T.; Al-Laham, M. A.; Peng, C. Y.; Nanayakkara, A.; Gonzalez, C.; Challacombe, M.; Gill, P. M. W.; Johnson, B. G.; Chen, W.; Wong, M. W.; Andres, J. L.; Head-Gordon, M.; Replogle, E. S.; Pople, J. A. *Gaussian 98*, revision A.1; Gaussian, Inc.: Pittsburgh, PA, 1998.
- (56) Wachters, A. J. H. *J. Chem. Phys.* **1970**, *52*, 1033.
- (57) Hay, P. J. *J. Chem. Phys.* **1977**, *66*, 4377.
- (58) Raghavachari, K.; Trucks, G. W. *J. Chem. Phys.* **1989**, *91*, 1062.
- (59) (a) Foresman, J. B.; Frisch, M. *Exploring Chemistry with Electronic Structure Methods*, 2nd ed.; Gaussian, Inc.: Pittsburgh, PA, 1996. (b) Koch, W.; Holthausen, M. C. *A Chemist's Guide to Density Functional Theory*, 2nd ed.; Wiley-VCH: Weinheim, Germany, 2001.
- (60) (a) Glendening, E. D.; Reed, A. E.; Carpenter, J. E.; Weinhold, F. *NBO 3.1*. (b) Reed, A. E.; Curtiss, L. A.; Weinhold, F. *Chem. Rev.* **1988**, *88*, 899.
- (61) Frenking, G.; Pidun, W. *J. Chem. Soc., Dalton Trans.* **1997**, 1653.
- (62) Dewar, M. J. S. *Bull. Soc. Chim. Fr.* **1951**, *18*, C71.
- (63) Chatt, J.; Duncanson, L. A. *J. Chem. Soc.* **1953**, 2939.
- (64) Sweany, R. L. *Inorg. Chem.* **1982**, *21*, 752.
- (65) Sweany, R. L.; Russell, F. N. *Organometallics* **1988**, *7*, 719.